COBEM 2021 26th International Congress of Mechanical Engineering
November 22-26, 2021, Virtual Congress, Brazil

COB-2021-2344
DESIGN OF A REGENERATIVE BRAKING SYSTEM FOR A BICYCLE DRIVEN BY AN ELECTRIC MOTOR OF 500 W

Luis André Vilcahuamán Hinostroza
Julio Cesar Cuisano Egúsquiza
Pontificia Universidad Católica del Perú, Lima, Perú
a20130623@pucp.edu.pe
jcuisano@pucp.edu.pe

Abstract. *Lima, the capital city of Peru, has a large amount of internal combustion engine vehicles used for private, public, and heavy load transport. This contributes not only to the vehicles traffic congestions all along with the city but to unnecessary emissions and noise. An alternative solution for moving around the city, and reducing the impact of motor vehicles, is the use of small vehicles and free of emissions such as bicycles. Between 2012 and 2017, these two-wheeled vehicles have experienced a tendency of having electric motors for pedal assistance or direct drive, changing into electric bicycles. Using a bicycle with a direct drive electric motor becomes a great alternative for moving large distances without physical fatigue. However, the major problem is the limited capacity of the battery and the hours it takes to fully charge. This makes it critical to manage the energy as efficiently as possible, which leads to focusing on the loss of energy during the braking. This energy can be recovered by the use of a regenerative braking system. The subject of the present study is to establish the equations and mathematical models required for describing the dynamics of the main components of the system. After defining the characteristic parameters of the proposed system, and using the equations defined for its dynamics, the behavior of the system in various braking conditions has been evaluated by numeric simulation in MATLAB's Simulink. The results indicate that it is possible to recover up to 1.32 kJ braking from 25 km/h to 8 km/h in 11.25 seconds. However, the maximum deceleration obtained 0.481 m/s2 represents approximately half of the average deceleration of bicycles in driving cycles in urban areas as Lima.*

Keywords: *Regenerative braking system, BLDC Motor, Electric bicycle, Simulation*

1. INTRODUCTION

Lima is considered the third city in the world with the most traffic congestion, leading up to an average of 58% of extra time for every trip made. At a lower scale, vehicles like motorcycles or bicycles are also affected, braking constantly because of the usual traffic. However, these last vehicles turn out to be a short term solution for traffic congestion because they occupy less space, allowing them to take shortcuts, easily change direction and also travel up to 16km/h in traffic, more than automobiles that travel between 10-12 km/h (El Comercio, 2019). In addition, two-wheel vehicles turn out to be more energy efficient because they required less mass for moving a person (10 kg bicycle compared to a 1600 kg light vehicle, approximately).

With bicycles being more popular in the city and being aware of the energy loss that takes place through common brakes during constant deacceleration on traffic congestion, it can be observed that there is a possibility of recovering energy, which can be estimated by a driving cycle in urban conditions. The bicycle driving cycle study is used to determine the average values of velocity, acceleration, deceleration, and kinetic energy, between other parameters. These data provide the total recoverable energy during braking and allows us to determine the best way to recover it.

Different prototypes of electric regenerative braking systems for bicycles have been developed, which allows an electric motor to function as a generator through a circuit with power electronics elements. For example, the Salesian Polytechnic University of Cuenca, Ecuador, developed a regenerative braking system for a rear-wheel DC motor-driven bicycle, to increase its autonomy (Toral, 2019). The system developed, was mainly composed of the following elements: brushless DC motor or "BLDC", charge controller, DC-DC converter, and a lithium-ion battery. Two driving tests were carried out on the bicycle with the regenerative braking system implemented. Gained-distance to distance-traveled rates of 7% and 1% respectively were obtained, managing to slightly increase the autonomy of the bicycle.

The objective of this work is to design a regenerative braking system model that allows recovering energy during braking on a bicycle driven by an electric motor, making it possible to store it for future use. In this way, it will be possible to increase the autonomy of the bicycle, powered by an electric motor, reducing the number of times necessary to recharge

its batteries and the need to pedal to travel long distances. The design involves the development of a model that characterizes the dynamic behavior of the system and the analysis of its response through numerical simulation.

2. MATHEMATICAL MODEL

The theoretical foundations that describe the dynamic behavior of the regenerative brake system and its components will be established. The mathematical equations and models of the bicycle, the electric motor, the battery, and other electronic components involved in the system are detailed, defining the variables involved and explaining the assumed considerations.

2.1 Bicycle dynamics

The necessary equations are proposed to determine the dynamic behavior of the bicycle and to carry out the following calculations. In this way, it will be possible to observe in greater detail the variables involved that are necessary to be evaluated or found through experimentation. The front wheel is assumed as the driven wheel, which means that the motor will be found in it. The bicycle movement is produced solely by the front-driven wheel. The total mass of the bicycle and the rider is represented at their center of gravity. The effects of rolling resistance, friction on bearings, chains, or other moving parts are considered not significant. The free-body diagram of the bicycle is shown in Figure 1,

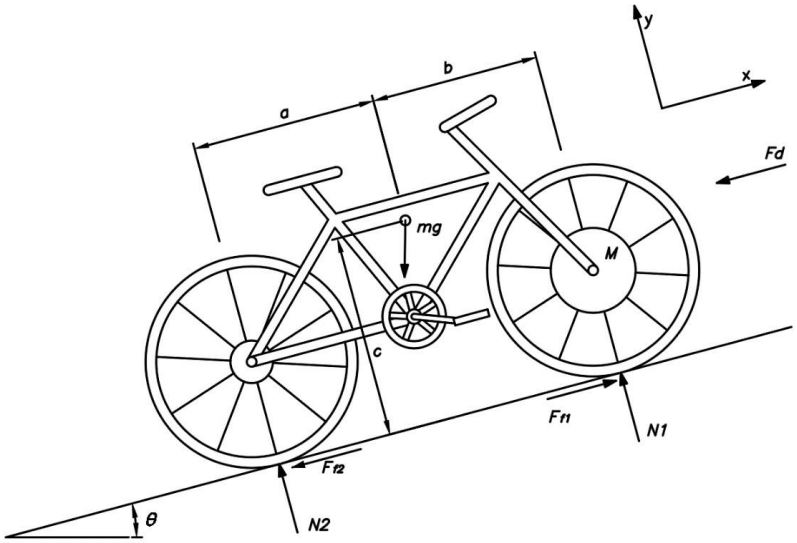

Figure 1. Free body diagram of a bicycle.

where $\boldsymbol{m}$, $\boldsymbol{g}$, $\boldsymbol{F_{fr1}}$, $\boldsymbol{F_{fr2}}$, $\boldsymbol{F_d}$, $\boldsymbol{N_1}$, and $\boldsymbol{N_2}$ are the total bicycle-driver mass (kg), gravity constant (m/s^2), friction force on the driven wheel (N), friction force on the rear wheel (N), air resistance force (N), the normal force on the driven wheel (N), and normal force on the rear wheel (N), respectively, and $\boldsymbol{a}$, $\boldsymbol{b}$, and $\boldsymbol{c}$ are the distances from the rear wheel to the center of mass (m), front-wheel to the center of mass (m), and floor to center of mass (m), respectively.

Applying Newton's second law on the x-axis, we obtain the following equation,

$$\boldsymbol{F_{fr1} - F_{fr2} - mg}\sin\theta - \frac{1}{2}.\boldsymbol{\rho}.\boldsymbol{A}.\boldsymbol{c_d}.\boldsymbol{v_x^2} = \boldsymbol{ma_x} \tag{1}$$

where $\boldsymbol{\rho}$, $\boldsymbol{A}$, $\boldsymbol{c_d}$, $\boldsymbol{v_x}$, and $\boldsymbol{a_x}$ are the air density (kg/m^3), front area of bicycle and driver (m^2), air friction coefficient, velocity in the x-axis (m/s), and acceleration in the x-axis (m/s), respectively.

Similarly, to determine the moments that intervene in the rotation of the driven wheel, a free-body diagram of the front wheel is shown in Figure 2, where $\boldsymbol{r_1}$, $\boldsymbol{T}$, $\boldsymbol{R_{1x}}$, $\boldsymbol{R_{1y}}$, $\boldsymbol{m_{r1}}$, and $\boldsymbol{I_{r1}}$ are the wheel radius (m), the torque applied by the electric motor (Nm), the reaction force of the bicycle structure on the x-axis (N), the reaction force of the bicycle structure on the y axis (N), front-wheel mass (kg), and moment of inertia (kg.m^2), respectively.

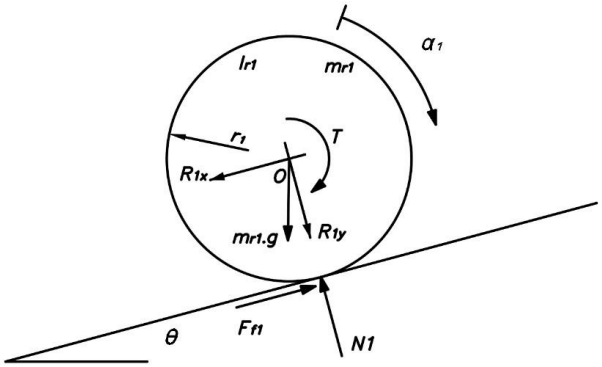

Figure 2. Free body diagram of the driven front wheel in the condition of rolling without slipping.

By this free body diagram, all forces and moments can be transferred to the axis of the electric motor, allowing the bicycle system and its variables to be reduced to one mathematical relationship. Applying Newton's second law on the x-axis, we obtain the following equation,

$$\boldsymbol{T - F_{f1}.r_1 = I_{r1}.\alpha_1} \tag{2}$$

In the same way, a free body diagram of the rear wheel is shown in Figure 3, where $\boldsymbol{r_2}$, $\boldsymbol{R_{2x}}$, $\boldsymbol{R_{2y}}$, $\boldsymbol{m_{r2}}$, and $\boldsymbol{I_{r2}}$ are the wheel radius (m), the reaction force of the bicycle structure on the x-axis (N), the reaction force of the bicycle structure on the y axis (N), rear-wheel mass (kg), and moment of inertia (kg.m^2), respectively.

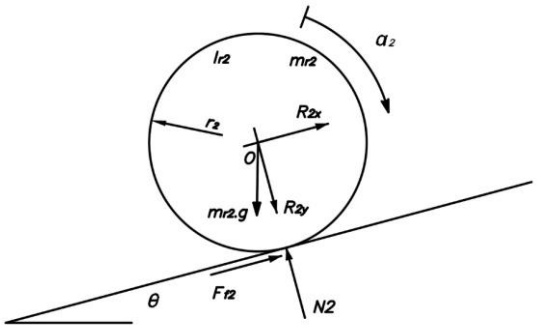

Figure 3. Free body diagram of the rear wheel in the condition of rolling without slipping.

Applying Newton's second law on the x-axis, we obtain the following equation,

$$\boldsymbol{F_{f2}.r_2 = I_{r2}.\alpha_2} \tag{3}$$

On the other hand, by the rolling condition, we have the following equations,

$$\boldsymbol{v_x}(t) = \boldsymbol{\omega}(t).\boldsymbol{r} \tag{4}$$

$$\boldsymbol{a_x}(t) = \frac{d\boldsymbol{\omega}(t)}{dt}.\boldsymbol{r} \tag{5}$$

Therefore, putting Eq. (1), (2), (3), (4), and (5) together, and considering that the radius of the front and rear wheels are the same, we obtain the following equation.

$$\boldsymbol{T}(t) - \boldsymbol{m.r.g}.\sin\theta - \frac{1}{2}.\boldsymbol{\rho.A.c_d.r^3.\omega^2}(t) = (\boldsymbol{m.r^2 + I_{r1} + I_{r2}}).\frac{d\boldsymbol{\omega}(\boldsymbol{t})}{dt} \tag{6}$$

In this last relation, we can observe the influence of the slope and the drag force of the air on the torque generated by the motor, as well as the equivalent inertia of the entire bicycle system towards the motor shaft.

2.2 DC Motor

The most used electric motors for light vehicles such as bicycles are permanent magnet DC motors because they can be powered directly by batteries, the speed is easily adjustable, they are compact and they have a low cost. The behavior of a DC motor can be represented through an electrical circuit in which three main components intervene: a resistance, an inductance, and an electromotive force. The electrical circuit of the DC motor is represented by the following equation,

$$\boldsymbol{V}(t) = \boldsymbol{R}.\boldsymbol{i}(t) + \boldsymbol{L}\frac{d\boldsymbol{i}(t)}{dt} + \boldsymbol{e_a} \tag{7}$$

where $\boldsymbol{V}$, $\boldsymbol{i}$, $\boldsymbol{R}$, $\boldsymbol{L}$, and $\boldsymbol{e_a}$ are the voltage of the source (V), electric current (A), resistance (Ω), and electromotive force (V), respectively.

According to (Mohan et al., 2009), the equations related to the electromotive force in a DC motor are:

$$\boldsymbol{V}(t) = \boldsymbol{R}.\boldsymbol{i}(t) + \boldsymbol{L}\frac{d\boldsymbol{i}(t)}{dt} + \boldsymbol{K_e}'.\boldsymbol{\omega}(t) \tag{8}$$

$$\boldsymbol{T_m} = \boldsymbol{K_e}'.\boldsymbol{i} \tag{9}$$

$$\boldsymbol{T_m}(t) = \boldsymbol{J_m}\frac{d\boldsymbol{\omega}(t)}{dt} + \boldsymbol{B_m}\boldsymbol{\omega}(t) + \boldsymbol{T}(t) \tag{10}$$

where $\boldsymbol{K_e}'$, $\boldsymbol{T_m}$, $\boldsymbol{J_m}$, and $\boldsymbol{B_m}$ are the back electromotive constant (V/Wb.rad/s), motor torque (Nm), motor moment of inertia (kg.m^2), and the damping coefficient (Nm/rad/s), respectively.

The damping coefficient depends on the friction losses in the mechanical components, mainly in the bearings. However, being a light and compact vehicle such as the bicycle, these frictional forces are insignificant and therefore were neglected for practical purposes. On the other hand, because the shaft of the electric motor is attached to the structure of the bicycle, the rotor becomes the outer part of the motor, which is attached to the wheel of the bicycle. Then, the moment of inertia of the rotor was considered as part of the moment of inertia of the wheel, which is already in the equation of the load torque. Therefore, Eq. (10) is reduced to the following form.

$$\boldsymbol{T_m}(t) = \boldsymbol{T}(t) \tag{11}$$

2.3 DC-DC Converter

The most common way to convert electrical voltage is with a transformer. The relationship between the input voltage of the primary circuit and the output voltage in the secondary circuit is given by the following equation,

$$\frac{\boldsymbol{I_1}}{\boldsymbol{I_2}} = \frac{\boldsymbol{E_2}}{\boldsymbol{E_1}} \tag{12}$$

where $\boldsymbol{I_1}$, $\boldsymbol{I_2}$, $\boldsymbol{E_1}$, and $\boldsymbol{E_2}$ are the current on the primary circuit (A), current on the secondary circuit (A), the voltage on the primary circuit (V), and voltage on the secondary circuit (V), respectively.

In the specific case of a DC-DC boost converter, required to raise the voltage generated by the motor for charging the batteries, the Eq. (13) can be considered (Mohan et al., 2009),

$$\frac{\boldsymbol{V_2}}{\boldsymbol{V_1}} = \frac{\boldsymbol{1}}{\boldsymbol{1-D}} \tag{13}$$

where $\boldsymbol{D}$ (a value between 0 and 1) is the duty cycle relation of the PWM signal that controls de DC-DC boost converter.

2.4 Battery

Batteries are essential for storing electrical energy in electric vehicles because they cannot be connected to a static power supply. A type of battery that has been in greater demand in recent years is the Lithium-Ion (Li-ion) battery. These batteries have the necessary qualities to be rechargeable, they have a high energy/weight ratio, longer useful life, low maintenance, minimal self-discharge, and low toxicity, unlike typical lead batteries. Tremblay & Dessaint (2019) proposed a battery dynamic model that can describe precisely the voltage and current dynamics. This model is shown in the following equation,

$$\boldsymbol{V_b = E_0 - R.i_b - K\frac{Q}{it - 0{,}1\,Q}.i_b^{*} - K\frac{Q}{Q - it}.it + A.e^{(-B.it)}} \tag{14}$$

where $\boldsymbol{V_b}$, $\boldsymbol{E_0}$, $\boldsymbol{R}$, $\boldsymbol{i_b}$, $\boldsymbol{K}$, $\boldsymbol{Q}$, $\boldsymbol{it}$, $\boldsymbol{A}$, $\boldsymbol{B}$, and $\boldsymbol{i_b^{*}}$ are the battery voltage (V), battery voltage constant, battery internal resistance (Ω), battery current (A), polarization constant, battery charge capacity (Ah), battery charge (Ah), exponential zone amplitude, exponential zone time constant, and battery filtered current (A), respectively.

3. REGENERATIVE BRAKING SYSTEM DESIGN

Numerical simulation is a widely used tool to analyze the behavior of physical systems, taking advantage of the great information processing capacity of computers. This allows checking the operation of proposed systems, obtaining results in a short time, and observing the capabilities of the system to carry out an optimal design. The process followed to simulate the regenerative brake system in the SIMULINK program of MATLAB is presented in this section.

3.1 Simulink blocks

The simulation of the regenerative braking system was carried out with SIMULINK from MATLAB. This program allows you to work with blocks that simulate components or real machines so that they can be connected to more complex systems. First, the blocks needed to build the system were selected. As an example, the "Vehicle body" block is shown in Figure 4. This block represents the main parameters of a two-axle vehicle (front and rear), considering the drag resistance of the air and the slope of the ground. From the SIMULINK gallery, the "Tire", "DC Motor" and "Battery" blocks were used and their respective input parameters were set.

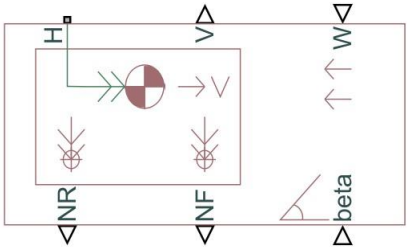

Figure 4. SIMULINK's Vehicle Body block (MathWorks, 2018).

Because no predetermined block meets the necessary characteristics to simulate the behavior of the DC-DC converter subsystem, a block was created in SIMULINK to meet the following equations of a DC-DC boost converter,

$$\boldsymbol{V_b = \left(\frac{1}{1 - D}\right)} \tag{15}$$

$$\boldsymbol{V_m.I_m = V_b.I_b} \tag{16}$$

where $\boldsymbol{D}$, $\boldsymbol{V_m}$, $\boldsymbol{I_m}$, $\boldsymbol{V_b}$, and $\boldsymbol{I_b}$ are the duty cycle of the DC-DC boost converter, motor side voltage (V), motor side current (I), battery side voltage (V), and battery side current (I), respectively. These relationships imply an ideal behavior of the converter, where there are no power losses. However, it is useful to observe its behavior and evaluate the performance of the system under different conditions. The DC-DC converter block made in SIMULINK is shown in Figure 5.

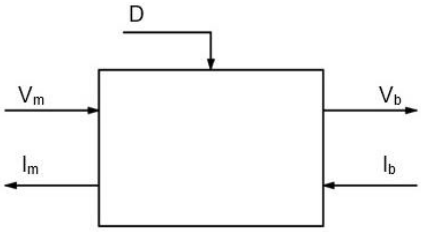

Figure 5. DC-DC boost converter block.

The simulation model developed was based on a 26-inch wheel bicycle with a 36V 500W BLCD motor and a 36V 13Ah battery, which characteristics and necessary constant values were obtained from Matthew Cain, S. (2013), Debraux *et al.* (2011)., Godfrey, A. J. *et al.* (2018), Asgari, S. *et al.* (2020), Beck, R. F. (2004), EEMB Co., L. (2010), Wong, J. Y. (2008), Rojas Chávez, F. (2016), Amazon (n.d) and others.

3.2 Braking system limitations

The maximum speed of the bicycle, taking as reference the specifications of the 36V and 500W BLDC motor, is 25 km/h (YescomUSA, n.d.). Considering this limitation, the maximum voltage that the electric motor could produce will be defined, considering the wheel radius and an electric motor constant K'e, as 24.7 V. The minimum voltage that the system can receive will be limited by the conditions of DC-DC boost converter input. A converter with 4.5-32 V and 5-42 V input and output range, respectively, will be considered as a reference for a real DC-DC boost converter (Drok, n.d.). From this information has been established that the minimum operating speed of the system is 5 km/h, which corresponds to 4.9 V on the motor side, taking into account the wheel radius and the electrical constant of the motor K'e.

On the other hand, the maximum and minimum voltage of the battery when its state of charge (SOC) is 100% and 0% is considered as 42 V and 32 V, respectively, taking as reference a Li-ion battery of 36 V and 13 Ah from Topex. From the voltage ranges on the motor side and the battery side, the need for a DC-DC boost converter can be seen. This is because the voltage must always be raised so that the battery can be charged.

3.3 System control module

Considering the established limitations, the operating range of the regenerative brake system is between 25 km/h, maximum velocity for bicycles in urban conditions (Toral, 2019), and 5 km/h, which corresponds to a range of voltages on the motor side from 24.7 V to 4.9 V, respectively. Outside of this voltage range, the regenerative braking system will be disconnected and the motor will be in an open circuit, running at no load. Since both the motor voltage and the battery voltage are variable, it is necessary to control the DC-DC boost converter to safely charge the battery. The maximum value of the charge current will be considered as the value of the fast charge current of the reference Li-ion battery, which corresponds to 6.5 A (Topex, n.d.).

To obtain the behavior of a conventional brake (constant deceleration) is necessary to obtain a constant torque, which implies a constant current on the motor side and a decreasing current on the battery side. One way to achieve this, and taking advantage of the decreasing voltage of the electric motor as the speed decreases, is by relating these two variables through a constant K. Considering that the maximum voltage on the motor side is approximately 25 V and the maximum current on the battery 6.5 A, the constant K that relates these variables is the ratio between these two values. Therefore, the value of K is 0.26, and Eq. (17) is set on the control module. The voltage in the motor and the expected current in the battery as a function of time, for a general braking situation, can be seen in Figure 6.

$$\boldsymbol{I_b} = 0.26\,\boldsymbol{V_m} \tag{17}$$

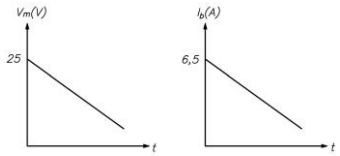

Figure 6. Motor voltage vs time (left) and desired battery current vs time (right).

The general block diagram of the system, which shows how the components, the main variables of the system, and the closed-loop control with feedback are related, is shown in Figure 7.

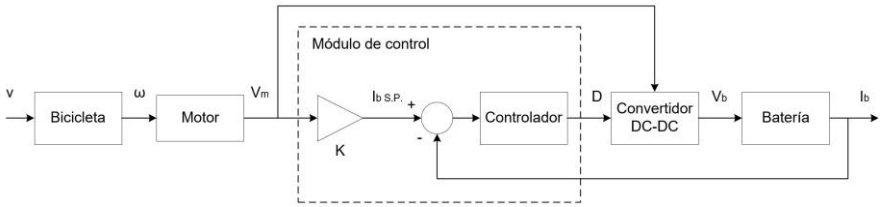

Figure 7. Block diagram of the regenerative braking system.

Due to the non-linear characteristics of the battery model, as well as considering an ideal behavior of the DC-DC converter, it is not possible to directly determine the transfer functions that define the behavior of these two subsystems to obtain and analyze the total transfer function of the system. However, by having their mathematical models, these blocks can be simulated to evaluate their behavior. Taking the above into account, a PID controller was used to perform the feedback control loop. The PID block (s) represents a transfer function shown in Eq. (17).

$$\boldsymbol{PID}(s) = \boldsymbol{P} + \boldsymbol{I}\frac{1}{s} + \boldsymbol{D}\frac{\boldsymbol{N}}{1 + \boldsymbol{N}\frac{1}{s}} \tag{17}$$

where $\boldsymbol{P}$, $\boldsymbol{I}$, $\boldsymbol{D}$, and $\boldsymbol{N}$ are the proportional, integral, derivative terms, and filter coefficients, respectively. To determine the PID values, the error was experimentally analyzed in SIMULINK, testing the control loop with an ideal linear descending voltage input between 25 V and 5 V, which would represent the voltage generated by the DC motor when braking. Different values were tested, starting from the simplest solution, first using only one proportional parameter and then adding another if necessary. Testing different values, it was determined that using only the values P = 20 and I = 40 would be enough to simulate the system control loop. A maximum error of 0.3% was obtained with these values.

4. RESULTS

After having developed the block system, we proceeded to build the block system in SIMULINK to simulate the system under different conditions. The model developed can be seen in detail in Figure 8. The battery effect on the motor side is represented through a variable resistor, whose numerical input signal Rm is calculated within the DC-DC converter block. Because this subsystem has an internal signal division block, when the program begins to iterate to simulate the system, it indicates an error because, in the first iterations, it encounters a division by zero that does not converge to a determined value. To overcome this drawback, the Rm output of the controller is not connected directly to the variable resistor. Instead, the "Repeating Sequence Interpolated" block is used, which generates a signal defining a certain number of points and interpolating the intermediate values. This block will be configured to obtain the resistance profile obtained at the converter output so that the motor current signal calculated in the converter matches the current signal measured in the motor.

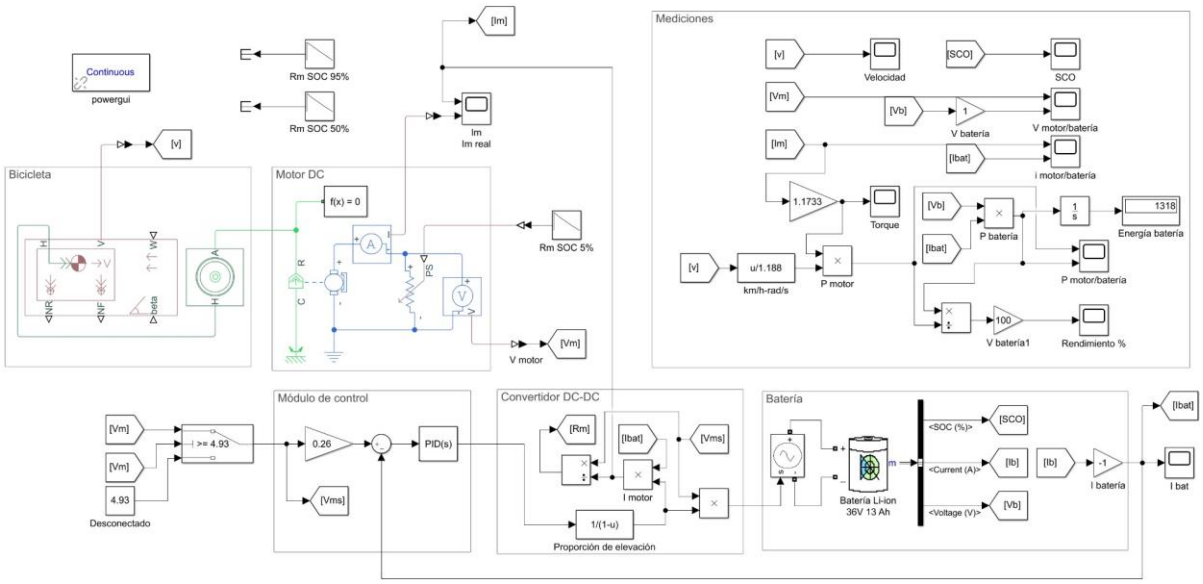

Figure 8. Regenerative brake system model in SIMULINK.

Considering the limits established for the regenerative braking system, three braking cases were simulated. The simulation begins with the bicycle at the maximum speed of 25 km/h, braking until reaching the minimum speed of 5 km/h, for an initial battery charge of 5%, 50 %, and 95%. To determine the instant when the system reaches minimum speed, the Switch block is used at the control module input, so the signal from the motor voltage sensor only enters the control module if it is greater than or equal to 4.93 V. If it is less, a constant signal of 4.93 V will be input.

The results obtained for Case 1, with an initial state of charge of the battery of 5%, are shown. Figure 9(a) shows the decreasing velocity of the bicycle with an average deceleration of 0.419 m/s^2. Figure 9(b) shows the motor and battery voltage, where the proportional relation of the bicycle velocity and the motor voltage can be seen. Figure 9(c) shows the motor braking torque, which is relatively constant at 10.8 Nm. Figure 9 (d) shows the battery and motor current, which is decreasing on the battery side and relatively constant on the motor side, as expected as the motor braking torque is proportional to the motor current. Table 1 shows the main results obtained.

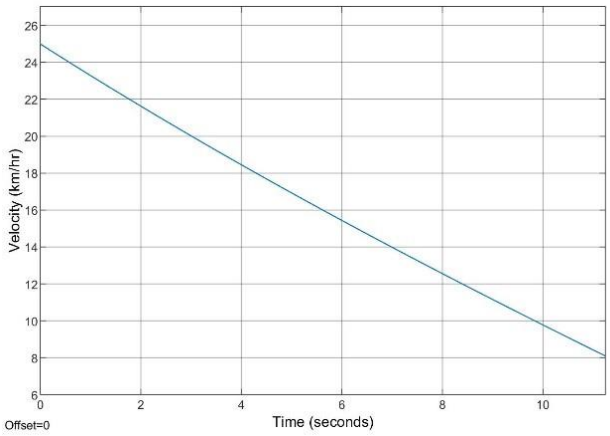

Figure 9(a). Bicycle velocity vs time.

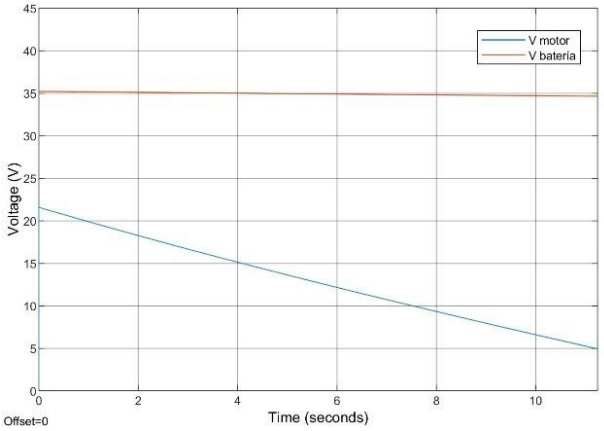

Figure 9(b). Motor and battery voltage vs time.

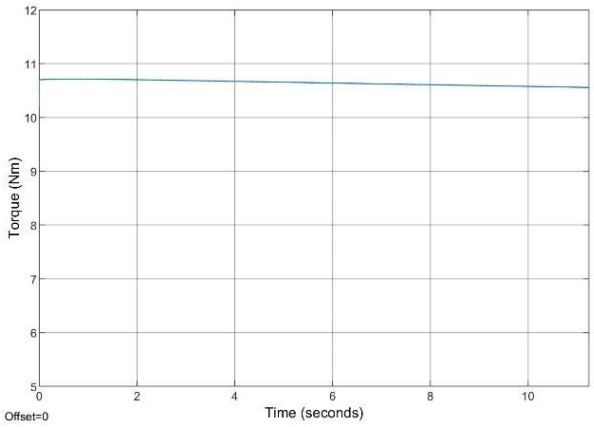

Figure 9(c). Motor braking torque vs time.

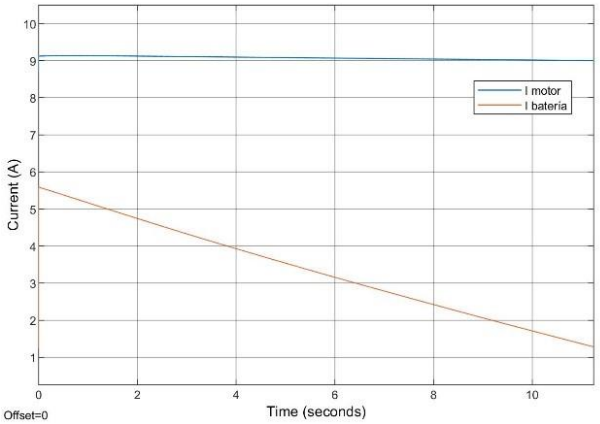

Figure 9(d). Motor and battery current vs time.

Table 1. Main results of the Regenerative Braking System simulation on SIMULINK for Case 1.

Variable	**Results**
Final SOC of battery, %	5.081
Total brake time, s	11.25
Total recovered charge, Ah	0.01053
Total recovered energy, J	1 318
Average deceleration, m/s^2	0.419

5. CONCLUSIONS

The simulation of the regenerative braking system developed in SIMULINK shows that it is possible to recover up to 1318 J, braking from 25 km/h to 8 km/h in 11.25 seconds, with the battery at 5% of its capacity. For these conditions, a constant brake torque of 10.8 is achieved. However, the maximum deceleration obtained 0.481 m/s^2, turns out to be approximately half of the average deceleration of bicycles in driving cycles in urban areas, which corresponds to 0.841 m/s^2 (Molina & Torres, 2016). This is mainly due to the battery limitations related to the maximum charge current, a value that is directly proportional to the maximum brake torque.

The system was developed considering an ideal DC-DC boost converter. For the system to work on a prototype, is necessary to design a converter that behaves as described in this work. On the other hand, the brake torque achieved is relatively constant, which was considered to obtain a similar behavior to the common bicycle braking case. However, the torque should be adjustable according to the driver's requirements. This can be achieved by modifying the control circuit in such a way that the desired torque is obtained regardless of the state of charge of the battery and the speed of the motor.

6. REFERENCES

Amazon. (n.d.). *JAXPETY 36V 500W Electric Bicycle Cycle 26" E Bike Front Wheel Ebike Hub Motor Conversion Kit Hub Motor Wheel*. Retrieved September 4, 2019, from https://www.amazon.com/JAXPETY-Electric-Bicycle-Cycle- Conversion/dp/B0761QYCKM/ref=sr_1_1?keywords=front+wheel+ebike+36v&qid=1567576656&s=gateway&sr=8-1

Beck, R. F. (2004). *Mountain Bicycle Acceleration and Braking Factors*. http://citeseerx.ist.psu.edu/viewdoc/download?doi=10.1.1.466.2501&rep=rep1&type=pdf

Debraux, P., Grappe, F., Manolova, A. V., & Bertucci, W. (2011). Aerodynamic drag in cycling: Methods of assessment. Sports Biomechanics, 10(3), 197–218. https://doi.org/10.1080/14763141.2011.592209

Drok. (n.d.). *DC 4.5-32V to 5-42V Boost Step-Up Converter Car Laptop Notebook Voltage Power Converter Wide Voltage Regulator*. Retrieved September 5, 2019, from https://www.droking.com/dc-4.5-32v-to-5-42v-boost-step-up-converter-car-laptop-notebook-voltage-power-converter-wide-voltage-regulator

EEMB Co., L. (2010). *Lithium-ion Battery DATA SHEET*. https://www.ineltro.ch/media/downloads/SAAItem/45/45958/36e3e7f3-2049-4adb-a2a7-79c654d92915.pdf

El Comercio. (2019, June 8). *Lima es la tercera ciudad del mundo con más congestión vehicular sobre otras 400 | Lima | Transporte | El Comercio Perú*. https://elcomercio.pe/lima/transporte/lima-tercera-ciudad-mundo-congestion-vehicular-400-noticia-ecpm-642900

Godfrey, A. J., & Sankaranarayanan, V. (2018). A new electric braking system with energy regeneration for a BLDC motor driven electric vehicle. Engineering Science and Technology, an International Journal, 21(4), 704–713. https://doi.org/10.1016/j.jestch.2018.05.003

Matthew Cain, S. (2013). *An Experimental Investigation of Human/Bicycle Dynamics and Rider Skill in Children and Adults* [University of Michigan]. https://deepblue.lib.umich.edu/bitstream/handle/2027.42/98003/smcain_1.pdf?sequence=1

MathWorks. (2018). *MATLAB R2018b*.

Mohan, N., M. Undeland, T., & P. Robbins, W. (2009). *Electrónica de Potencia-Convertidores, aplicaciónes y diseño* (3ra Edició). McGraw Hill.

Molina, F. D., & Torres, J. C. (2016). *Determinación del ciclo típico de conducción de una bicicleta en las ciclovías de la ciudad de Cuenca* [Universidad del Azuay]. http://dspace.uazuay.edu.ec/handle/datos/6350

Rojas Chávez, F. (2016). *TABLAS TERMODINÁMICAS*.

Topex. (n.d.). *China 36V 13Ah Little Frog Li-ion Battery For Elelectric Bicycle*. Retrieved September 4, 2019, from http://www.topexbattery.com/electric-vehicle-battery/electric-bicycle-battery/36v-13ah-little-frog-li-ion-battery-for-elelectric.html

Toral, J. D. (2019). *Desarrollo del freno regenerativo en un motor sin escobillas para una bicicleta*. Universidad Politécnica Salesiana.

Tremblay, O., & Dessaint, L.-A. (2009). *Experimental Validation of a Battery Dynamic Model for EV Applications*. https://pdfs.semanticscholar.org/8f16/68ffef08c83a3a69f8f3c557d04cd9a5ffc2.pdf

Wong, J. Y. (2008). Theory of ground vehicles. Wiley.

YescomUSA. (n.d.). *Brushless Electric Bicycle Engine, 36v 500w Front Wheel Hub Motor Kit*. Retrieved September 4, 2019, from https://www.yescomusa.com/products/brushless-electric-bicycle-engine-36v-500w-front-wheel-hub-motor-kit

7. RESPONSIBILITY NOTICE

The authors are the only ones responsible for the printed material included in this paper.